

MODELING AND EXPERIMENT ANALYSIS OF VARIABLE REFRIGERANT FLOW AIR-CONDITIONING SYSTEMS

Xuhui Wang¹, Jianjun Xia¹, Xiaoliang Zhang¹, Sumio Shiochi², Chen Peng¹, Yi Jiang¹

¹Department of Building Science, Tsinghua University, Beijing, China

²Environmental Technology Lab., Daikin Industries, Ltd., Osaka, Japan

ABSTRACT

This study developed a component-based gray-box model for variable refrigerant flow (VRF) air-conditioning systems to simulate and predict the performance and energy consumption of VRF system in cooling condition. Results from the testing of Daikin's 10HP VRV system with six indoor units, as well as the manufacturer's data, were used to fit the key parameters of each component in this VRF model. This model was integrated in the building energy simulation software *DeST* and was validated by using data both from Daikin's product handbook and from tested results. The validation results showed that this model can be used to calculate the coefficient of performance (COP) of VRF systems in an error of less than 15%.

KEY WORDS

VRF, gray-box model, simulation, experiment

INTRODUCTION

Variable Refrigerant Flow (VRF) air-conditioning system is a type of newly widely used system, due to its flexibility and high coefficient of performance (COP) in part load conditions comparing with traditional central air-conditioning systems. There are one or more variable-frequency compressors in a VRF system so that the capacity can be adjusted by varying the compressor's frequency to match with the change of the thermal load. The indoor units in a VRF system can be independently controlled by varying the refrigerant flow rate to meet the cooling or heating requirement in each room, so VRF system is especially suited for the kind of building with different functional rooms and complicated load conditions, such as office buildings and market buildings.

However, the real performances of VRF systems in buildings are usually not as good as what are described by manufacture's data, mainly because of improper design of outdoor unit and indoor units, the ignorance of the influences of refrigerant pipe length and gravity when there's large difference in altitude between different units in the system. To reach a higher performance, a careful design is needed from

the very beginning, and all-condition simulation is a quite powerful method to check the performance of VRF system in all kinds of working conditions so as to provide plenty of data as a reference for the system design.

Among the building energy simulation tools in the world, only *EnergyPlus* contains a VRF calculation module, which was developed by Zhou, Y. P. in 2006. The VRF model in *EnergyPlus* is a curve-based black-box model in which most of the coefficients were fitted from manufacturer's data and then formed almost pure mathematical formulas with little physical meaning, to present the performance curve of VRF systems. This kind of model has fast calculating speed and high accuracy, but can not reflect the performance of each component of VRF system in different load conditions, and the extensibility of the model is quite limited because all the fitting work should be carried out once more to represent the properties of a new VRF system.

This study developed a component-based gray-box VRF model and integrated it in the building energy simulation software *DeST*, developed by Tsinghua University, China. Compared with the VRF model in *EnergyPlus*, this gray-box model can reflect the performances of each component and only several key parameters were needed to be re-identified to represent the characteristics of different VRF systems. Moreover, this kind of gray-box model is quite suited for hour-step all-condition simulation, which is the same simulation time interval applied in *DeST*. The model was validated by the manufacture's data of Daikin as well as the experimental results of Daikin's 10HP VRV system in Tsinghua University.

VRF MODELING METHODOLOGY

The model of VRF system is a component based gray-box model, in which the compressor, the outdoor heat exchanger and fan, the indoor heat exchanger and fan and the throttle valve are modelled with gray-box method, and they are solved simultaneously with a single-phase flow model for the refrigerant pipe network.

The compressor model is a typical model of vortex compressor, which is referred to Xia, J. J.'s research in his doctoral thesis in 2005. The working process of a vortex compressor can be divided into three processes, as shown in Figure 1:

1) Preheating in the suction of the compressor. The heat loss from the motor preheats the refrigerant before it goes inside the suction zone (su->su1).

2) Isotropic compressing process (su1->ex1). This process is first in constant entropy then in constant volume, divided by the adoption point (see "ad" point in Figure 1), whose refrigerant volume was determined by the volume in the suction $v_{su1,cp}$ and the interior compressing ratio π_v :

$$v_{ad,cp} = v_{su1,cp} / \pi_v \quad (1)$$

3) Cooling in the air exhausting opening (ex1->ex). The energy consumption of the compressor is given by the ideal compressing power \dot{W}_{in} and its relationship with the actual power \dot{W}_{cp} :

$$\dot{W}_{in} = \dot{M}_{cp}(h_{ad,cp} - h_{su1,cp} + v_{ad,cp}(p_{ex,cp} - p_{ad,cp})) \quad (2)$$

$$\dot{W}_{cp} = \dot{W}_{loss} + \alpha_1 \dot{W}_{in} + \alpha_2 \dot{W}_{in}^2 \quad (3)$$

The compressor frequency is determined by the swept volume v_{sw} and the volume efficiency ε_v :

$$f = M_{ref,cp} v_{su1,cp} / (v_{sw} \varepsilon_v) \quad (4)$$

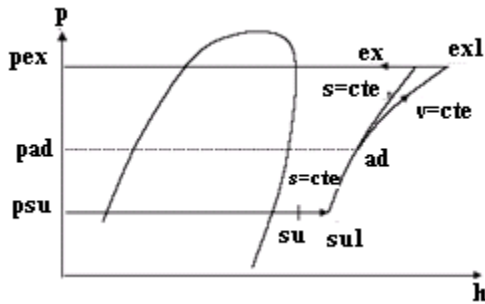


Figure 1 working process of the vortex compressor

For the heat exchangers (HEX), they are divided into two or three zones according to the refrigerant state, and the lumped parameter method were applied in each zone. In cooling condition, the outdoor heat exchanger is the condenser, which includes the super-heating zone, the two-phase zone and the sub-cooling zone, as shown in Figure 2. The indoor heat exchangers are the evaporators, which only include the two-phase zone and the super-heating zone, as shown in Figure 3. Each zone was regarded as a counter-flow heat exchanger and the ε -NTU method was applied to calculate the heat exchanging capacity in each zone. Taking the super-heating zone as an example, the heat exchanging capacity was calculated by the following equations:

$$AU_{sh} = \alpha_{sh} / (R_{sh} + R_a) \quad (5)$$

$$NTU_{sh} = AU_{sh} / \min((\dot{m}c)_{sh}, (\dot{m}c)_a) \quad (6)$$

$$\omega = \frac{\max((\dot{m}c)_{sh}, (\dot{m}c)_a)}{\min((\dot{m}c)_{sh}, (\dot{m}c)_a)} \quad (7)$$

$$\varepsilon_{sh} = \frac{1 - \exp(-NTU_{sh}(1 - \omega))}{1 - \omega \exp(-NTU_{sh}(1 - \omega))} \quad (8)$$

$$\dot{Q}_{sh} = \varepsilon_{sh} \min((\dot{m}c)_{sh}, (\dot{m}c)_a) (t_{a,su} - t_{sh,su}) \quad (9)$$

α_{sh} is the area ratio of the super-heating zone in the whole heat changer. It's the same to calculate the heat exchanging capacity in the two-phase zone and the sub-cooling zone.

The heat transfer in the two-phase zone is boiling heat transfer, while in the super-heating zone and sub-cooling zone it is mainly convective heat transfer. So the relationships of the thermal resistances in different zones were estimated as: $R_{sh} = 10R_{tp}$, $R_{sc} = 8R_{tp}$. The thermal resistances in the air side and in the refrigerant side change with the air volume and refrigerant flow rate, which are presented by the following equations:

$$R_{tp} = (\dot{m}_{ref,n} / \dot{m}_{ref})^{0.8} R_{tp,n} \quad (10)$$

$$R_a = (\dot{m}_{a,n} / \dot{m}_a)^{0.6} R_{a,n} \quad (11)$$

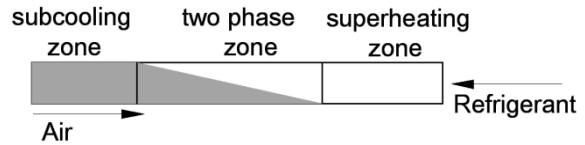


Figure 2 zone division of the condenser

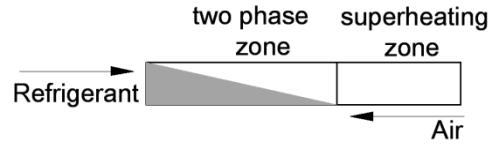


Figure 3 zone division of the evaporator

The throttle valve was modelled as an idealized throttling device so that the refrigerant enthalpies before and after the throttle valve are the same:

$$h_{su,v} = h_{ex,v} \quad (12)$$

The energy consumption of outdoor unit fan is related with the cooling amount and ambient temperature, so that its energy consumption $\dot{W}_{ou,fan}$ was fitted as the function of the two factors:

$$\dot{W}_{ou,fan} = a + b\dot{Q}_{cooling} + ct_{amb} + d\dot{Q}_{cooling}^2 + et_{amb}^2 + f\dot{Q}_{cooling}t_{amb} \quad (13)$$

For the indoor unit fan, thinking of a simplified situation that the users won't switch it between high speed and low speed, it will keep operating in its nominal electric power (at high speed) as long as it is opened up and won't stop even when the throttle valve is shut down. So the power of the indoor unit fan equals to its nominal power during the operating time of VRF system:

$$\dot{W}_{iu,fan} = \dot{W}_{iu,fan,n} \quad (14)$$

The refrigerant in the pipes connecting different components in the VRF system are mostly in single phase, either gas or liquid, so a single phase refrigerant flow model was applied here. The pressure drop in the pipes was calculated as following:

$$\Delta p_{pipe} = f \frac{L}{d_i} \frac{v_r^2}{2} \rho_{ref} \quad (15)$$

f is the friction factor which was estimated according to Colebrook's friction factor equation in 1944:

$$\frac{1}{\sqrt{f}} = 1.14 + 2 \log\left(\frac{1}{\frac{\epsilon}{D}}\right) - 2 \log\left(1 + \frac{9.3}{R_e \cdot \frac{\epsilon}{D} \cdot \sqrt{f}}\right) \quad (16)$$

$$f = 64/R_e \quad (R_e < 2100) \quad (17)$$

ϵ is the roughness of the pipe inner surface, which is 10^{-5} m in this case. R_e is the Renault value of the refrigerant flow.

Control strategy is quite important to the performance of the VRF system. Daikin provided the overall control strategy of the system and it was applied in this model. Basically the indoor units were controlled independently, varying their refrigerant flow rates by varying the openings of the throttle valves to meet the cooling/heating demands of each room. The evaporating temperature is controlled at 6 degree by varying the compressor's frequency. In the indoor unit side, the exhausting refrigerant super-heating temperature is set at 5 degree. In the outdoor unit side, the exhausting sub-cooling temperature is controlled at 5 degree. Meanwhile, there's a bypass refrigerant flow from the outlet of the outdoor heat exchanger back to the inlet of the compressor to control the inletting super-heating temperature of the compressor.

In this component-base gray box model, the feature of a VRF system is determined by the key parameters of the model, so that they have to be identified first to reflect the characteristics of the real system. Some of the key parameters were provided directly by Daikin while the others needed to be fitted by using the manufacturer's performance data. Daikin provides totally 21 types of VRV systems' parameters, from 8HP to 48HP. Taking the system RHXYQ10PY1 (10HP) as an example, the parameters provided by Daikin directly are shown in Table 1:

Table 1
Parameters of Daikin's RHXYQ10PY1 system

Refrigerant: R410A
Internal compressing ratio $\pi_v = 2.75$
Swept volume $v_{sw} = 0.00006m^3$
Nominal thermal resistance in the air side $R_{a,n} = 0.16728W/K$
Nominal thermal resistance in the refrigerant side in two phase zone $R_{tp,n} = 0.09208W/K$

The performance data were presented in the form of the energy consumption of compressor and the outdoor unit fan in different cooling part load ratio and ambient temperature, as shown in the following formula:

$$\dot{W}_{cp} + \dot{W}_{ou,fan} = f(\dot{Q}_{cooling}, t_{amb}) \quad (18)$$

The parameters related to the energy consumption of the compressor and outdoor unit fan were not given directly and their identification process is shown in Figure 4.

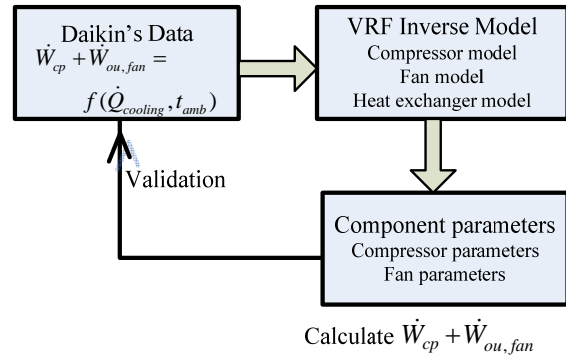


Figure 4 Parameter Identification Methodology

The energy consumption of the compressor and outdoor unit fan were calculated in a VRF inverse model, then they were expressed in the form of equation (3) and (13) with the parameters fitted, so as to be related with the results from the gray-box model. In equation (3), \dot{W}_{in} is calculated from the gray-box model and \dot{W}_{loss} , α_1 and α_2 are the fitted parameters of compressor. In equation (13), $\dot{Q}_{cooling}$ and t_{amb} are from the input of the gray-box model and the coefficients from a to f are the fitted parameters of outdoor unit fan.

The above fitted parameters of RHXYQ10PY1 are shown in Table 2. Because the manufacturer's data only cover the conditions when the part load ratio (PLR) is above 50%, the data in Table 2 is only suited for simulating the system performance of above 50% PLR conditions. According to Daikin's control strategy, in above 50% PLR condition, the outdoor unit fan always works in nominal frequency so $\dot{W}_{iu,fan} = \dot{W}_{iu,fan,n} = \frac{0.75}{\eta} = 1.071kW$. In this case, there is no need to fit the coefficients from a to f . So only the three parameters of compressor are shown in Table 2.

Table 2
Fitted Parameters of RHXYQ10PY1 by manufacturer's data

\dot{W}_{loss}	-0.39451	α_1	1.15785	α_2	-1.46052E-3
------------------	----------	------------	---------	------------	-------------

The calculating result of the total energy consumption of the compressor and outdoor unit fan ($\dot{W}_{cp} + \dot{W}_{ou,fan}$) by using the identified parameters were compared with the manufacturer's performance data, the relative errors are shown in Figure 5. Most of the relative errors are less than 5%, so that the model with identified parameters is accurate enough to be used to calculate the whole year performance of VRF system.

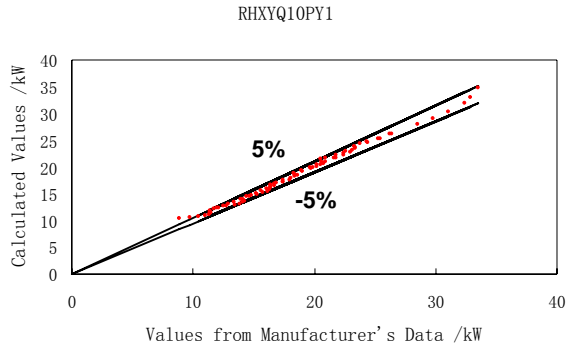


Figure 5 Identification Result of RHXYQ10PY1

As mentioned above, the manufacturer's data only covers the conditions when the part load ratio (PLR) is above 50%, and the simulation results will be inaccurate if we use the parameters identified by the above 50% PLR data to calculate the energy consumption when PLR is below 50%. So experiment of VRF system was introduced into this study to get the performance data in below 50% PLR conditions.

VRF TESTING METHOD

As mentioned above, in order to get real performance data as the supplementary of the performance data from the manufacturer and carry out future research on the performance of VRF system, a VRF testing bench was established in the Low Energy Demo Building of Tsinghua University. Seven climate chambers were used to generate both the indoor and outdoor environments. The tested VRF system is Daikin's 10HP VRV system with one outdoor unit (RHXYQ10PY1, nominal cooling capacity 28kW) and six indoor units (FXDP50MPVC, nominal cooling capacity 5kW).

The six indoor units were placed in from Chamber 2 to 7 as shown in Figure 6, whose dimensions are all 3.6m (Length)*3.6m (Width)*2.2m (Height). The enclosures of the chambers are made of 100mm insulation materials and their area overall heat transfer coefficients $AU_{amb,i}$ and $AU_{adj,i}$ were tested beforehand. There are variable-input-power electric thermal fins in the six chambers to generate the indoor heat gains, and their input power $\dot{Q}_{input,i}$ can be tested by real time electric power meters. The six chambers were kept well airtight during the experiments and anti-radiation materials were stuck on the surfaces of each chamber to eliminate the influence of solar radiation. The cooling load for each indoor unit $\dot{Q}_{iu,i}$ is calculated by room heat balance method:

$$\dot{Q}_{iu,i} + \dot{Q}_{input,i} + AU_{amb,i}(t_{amb} - t_{room,i}) + \sum_{j \neq i} AU_{adj,j}(t_{room,j} - t_{room,i}) = 0 \quad (19)$$

The outdoor unit was placed in Chamber 1, with openings in the three external walls facing the three inlet areas of the outdoor unit respectively. There is a

variable-frequency fan on top of Chamber 1 to control the amount of outdoor air flowing through the openings of Chamber 1 and mixing with the hot air exhausting from the outdoor unit so as to control the inlet air temperature of the VRF system.

For the metering utilities, dozens of thermal couples were used to measure both the air temperatures and refrigerant temperatures, and totally 8 pressure sensors were placed in the inlet and outlet of the outdoor unit and the outlets of the 6 indoor units to measure the refrigerant pressure. There's a CORIOLIS mass flow meter in the outlet liquid pipe of the outdoor unit to measure the total refrigerant mass flow rate. Seven electric power meters were used to measure the energy consumption of the VRF system and the power input in chamber 2 to 7. All the measured data were recorded by computer every minute. Moreover, there's a "checker" provided by Daikin to record the system performance parameters every minute, including the frequency of the compressor and the openings of the throttle valves.

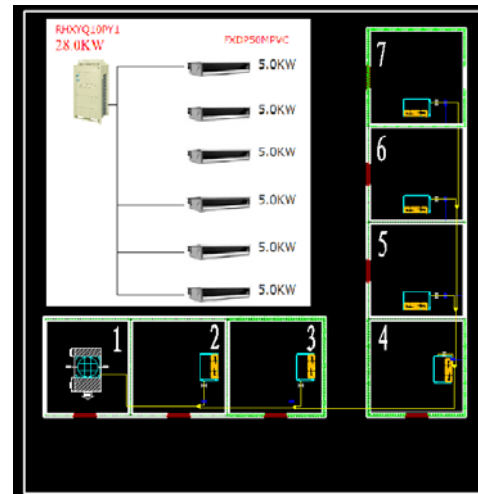


Figure 6

Layout of Experiment bench and VRF for testing

TESTING RESULT ANALYSIS

According to Manufacturer's data, the rated controlled room temperature range is $t_{set} \pm 1^\circ\text{C}$. However, since the thermal inertias of the climate chambers are smaller than ordinary rooms, the air temperatures changed faster in these climate chambers and the actual controlled room temperature range was about $t_{set} \pm 2^\circ\text{C}$, and the periodic time for the rising and falling of the temperature was around 10 minutes, as shown in Figure 7.

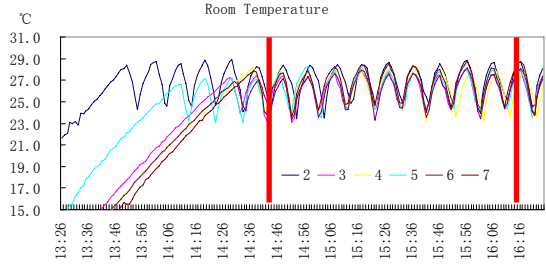
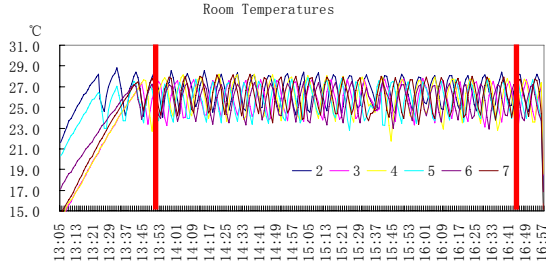


Figure 7 Tested six rooms' temperatures

From Figure 7 we can see that the VRF system wasn't in a pure stable stage but in different operating conditions from minute to minute, so the transient COP is meaningless to reflect the average performance of the VRF system. However, after tens of minutes from the starting time, the VRF system will operate in a kind of "dynamic stable" stage, in which the system's operating parameters changed periodically, such as the period between the two vertical lines in Figure 7. The six indoor units operated either at the same step or differently, which can be seen from the two pictures in Figure 7. The average COP calculated by data from this kind of dynamic stable stage can reflect the average performance of the VRF system. The average COP was calculated by the following formula (assuming the dynamic stable stage is from time 0 to time τ):

$$COP = \int_0^\tau \sum_{i=2}^7 \dot{Q}_{iu,i} / [\int_0^\tau (\dot{W}_{ou,cp} + \dot{W}_{ou,fan} + \sum_{i=2}^7 \dot{W}_{iu,fan,i})] \quad (20)$$

The part load ratio in the period was mainly determined by the input power of the electric fins, and also influenced by the heat transferring through the enclosures. It was defined as:

$$PLR = \frac{\int_0^\tau \sum_{i=2}^7 \dot{Q}_{iu,i}}{\tau \dot{Q}_{ou,n}} \quad (21)$$

The tested VRF COP results are shown in Figure 8, under the testing schemes shown in Table 4 in the appendix (at the end of this paper). When the part load ratio ranged from 18% to 65%, the COP values ranged from 1.8 to 4.0, and generally the COP values decreased with the decrease of PLR. In a certain part load ratio, the COP values were different with each other, mainly because the difference of ambient temperatures. The highest COP appeared between 40% and 50% PLR. These testing results show good consistency with the testing results of Daikin's VRV system by Zhou, Y. P. in Shanghai Jiao Tong University in 2007.

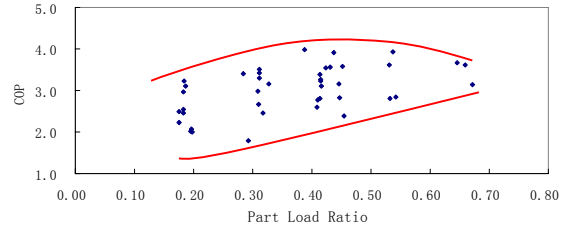


Figure 8 Tested VRF COP

In order to check how the system COP was influenced by the ambient temperature, we used the ambient temperature as the X axis in Figure 9, and those points who were in the similar part load ratio were put in a group. For example, the first 10 points from Table 4 whose PLR were all around 0.18 were put in a group, then the next 9 points whose PLR were all around 0.30 were put in another group. Figure 9 shows that generally the COP values decreased with the increase of ambient temperature, because higher ambient temperature led to higher condensing temperature. The situation that several points showed a different trend (COP increased when ambient temperature increased) was due to the testing error.

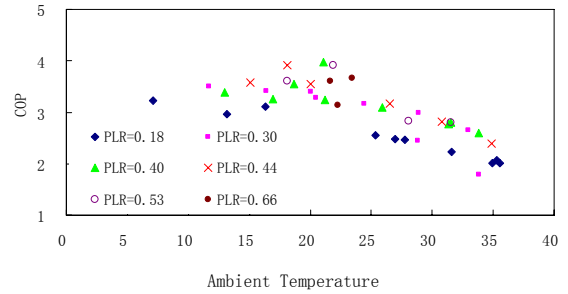


Figure 9 COP changes with the ambient temperature

In Figure 10, the tested COP values and the COP values from manufacturer's data were put together. Compared with the sample COPs, the tested COPs were lower, especially when PLR is from 50% to 65% where there was a direct comparison. One reason might be that the controlled results were not as good as it should be as mentioned above in figure 7, leading to the fluctuation of the system operating status and increasing the on-off losses. More information about the system detail of the sample data is also needed to correctly analyse the differences. The testing results from 100% PLR to 65% PLR are also needed to carry out further comparison of tested COP values and sample COP values.

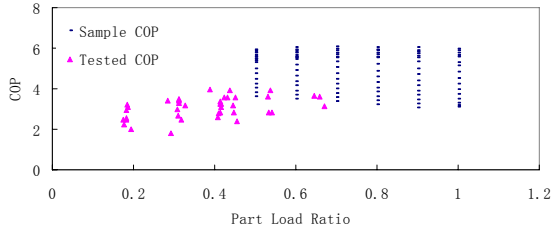


Figure 10 Tested VRF COP and sample COP

VRF MODEL VALIDATION AND APPLICATION

Using the tested data from 18% PLR to 55% PLR, the parameter identification process was carried out in the same way as described in Figure 4. That's to say, in the VRF performance simulation, when PLR is larger than 50% PLR (included) the parameters identified by manufacturer's data will be used, while when PLR is smaller than 50% (not included) the parameters identified by tested data will be used. The identified parameters for compressor and outdoor unit fan are shown in Table 3, corresponding to equation (3) and (13) respectively.

Table 3
Fitted Parameters of RHXYQ10PY1 by tested data

\dot{W}_{loss}	0.84358	α_1	1.30043	α_2	2.08872E-3
a	-1.9945E-01	b	5.5601E-02	c	7.6872E-03
d	2.2126E-03	e	-7.5478E-06	f	-3.7330E-04

Using the VRF model with the parameters identified from both manufacturer's data and tested data, the system COP values were calculated with the part load ratio ranging from 10% to 100%, and the ambient temperature ranging from 10 degree to 39 degree in each part load ratio. The simulation result of COP is shown in Figure 11. When the part load ratio decreases from 100% to 10%, the COP values first increase and then decrease, with the peak value appearing between 50% and 60% PLR. This trend shows good consistency with the characteristics of actual VRF system. However, because different source data were used for the parameter identification in below 50% PLR conditions and above 50% PLR conditions, there is a relatively sharp decrease when PLR changes from 50% PLR to 40% PLR. This problem should be solved by using the unified data source to identify the key parameters of the model, which means that more experimental data are needed to cover the above 50% PLR conditions in the future, and then only use the testing results for the parameter identification of the model.

The simulation result of COP was compared with manufacturer's data and tested data to validate the model. For the simulated COP values when PLR is larger than 50% PLR (included), they were compared with manufacturer's data. For the simulated COP values when PLR is smaller than 50% (not included),

they were compared with the tested data. The relative errors of the comparison are shown in Figure 12, the largest absolute value of the error is 18.15%, and most of them are less than 15%, indicating that this VRF model in *DeST* is good to estimate the VRF system's performances accurately.

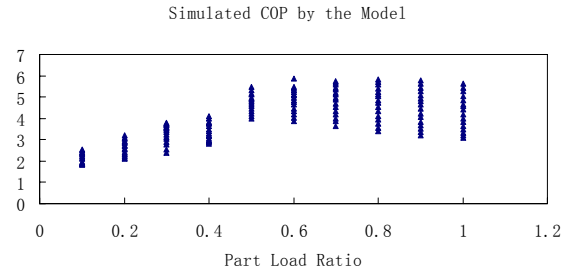


Figure 11 Simulated COP by the Model

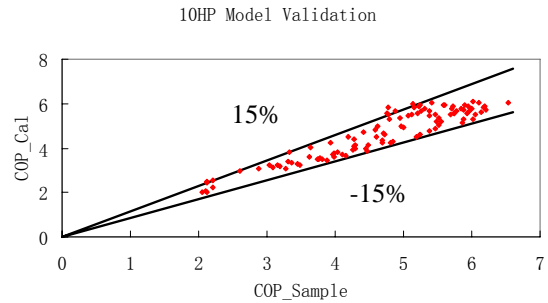


Figure 12 Model Validation

Using the validated model, the VRF simulation procedure in *DeST* is shown in Figure 13. The building load is first simulated in *DeST*, and then according to the load result the VRF systems will be designed. There already have been several tens of VRF products in *DeST*'s database whose key parameters have already been identified. The user will select the proper indoor units for each room according to the load of each room, and then select the proper outdoor unit according to the total load of the system. The positions of each indoor and outdoor unit, as well as each connecting node of the pipe network can be defined by inputting their 3-dimensional coordinates, so that the structure of the pipe network is determined. After that, the performance of VRF system will be simulated hour-by-hour, using hourly room load and room temperature as the input. The outputs are the energy consumptions of compressors, the outdoor unit fan and the indoor units of the VRF system, as well as the system COP values.

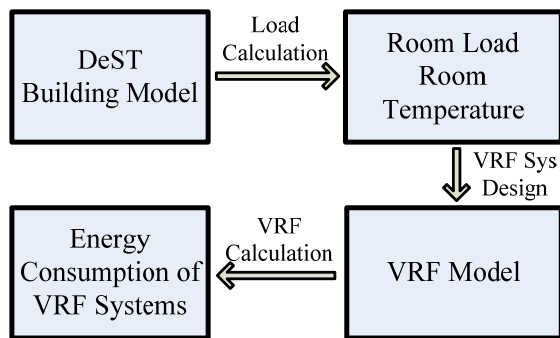


Figure 13 VRF Simulation Procedure in DeST

CONCLUSION AND DISCUSSION

This study built a component based gray-box VRF model in *DeST*. The model of vortex compressor, outdoor heat exchanger and fan, indoor heat exchanger and fan, throttle valve and single-phase pipe network were built respectively and then solved simultaneously. Data from Daikin's product handbook were used first to fit the key parameters of each component in above 50% PLR conditions, then the testing results of Daikin's 10HP VRV system were used to reflect the performance of VRF system in below 50% PLR condition, which was not presented in Daikin's data.

The key parameters of the model was fitted by using Daikin's performance data from 50% PLR (included) to 100% PLR and tested data below 50% PLR (not included). The validation result shows that most of the relative errors of calculated COP are within $\pm 15\%$, which indicated that the model of Daikin's 10HP VRV system can reflect the performance of the real system accurately.

Further work to improve this model will include more testing result to cover the performance of VRF system in more conditions and to check the reason for the differences between the tested data and manufacturer's data. In addition, how to properly extent the testing result of 10HP VRV system to other VRF systems needs further research.

REFERENCES

- Daikin Handbook for Equipment Design, VRV III SYSTEM (R410A). EDZS 06-4A. 2006.
- Moody L.F. 1944. Friction factors for pipe flow. ASME Trans. 663-672.
- Xia, J.J., 2005. Research on optimization control of the variable refrigerant flow (VRF) air-conditioning system. Ph. D. thesis. Tsinghua University. Beijing. China.
- Zhou, Y.P., Wu, J.Y. 2006. Energy simulation in the variable refrigerant flow air-conditioning system under cooling conditions. *Energy & Buildings* (2006), doi:10.1016/j.enbuild.2006.06.005.

- Zhou, Y.P., Wu, J.Y. 2007. Simulation and experimental validation of the variable-refrigerant-volume (VRV) air-conditioning system in EnergyPlus. *Energy & Buildings* (2007), doi:10.1016/j.enbuild.2007.04.025.

NOMENCLATURE

TEXT

AU	Area heat transfer coefficient
c	Specific heat
h	Enthalpy
\dot{m}	Mass flow rate
f	Compressor frequency
NTU	Number of transfer units
ω	The capacity rate ratio
p	Pressure
\dot{Q}	Heat flux
t	Temperature
\dot{W}	Electric power
x	Dryness of refrigerant
v	Specific volume
ε	Heat transfer efficiency
ρ	Density
R	Thermal resistance
α	Area ratio

SUBSCRIPT

ref	Refrigerant
a	Air
amb	Ambient air
ou	Outdoor unit
iu	Indoor unit
n	Nominal condition
cd	Condensing parameter
cp	Compressor
ev	Evaporating parameter
su	Supply (Inlet)
ex	Exhaust (Outlet)
fan	Fan
g	Gas
l	Liquid
sc	Sub-cooling
tp	Two phase
sh	Super-heating
$room$	Climate chamber
suc	The suction of compressor
v	Throttle valve
$pipe$	Refrigerant pipe
$cooling$	For cooling condition

APPENDIX

Table 4 Testing Schemes

PLR	Ambient temperature (°C)	COP
0.184	7.08	3.228
0.183	13.15	2.961
0.186	16.31	3.113
0.182	25.37	2.552
0.18	26.92	2.48
0.18	27.77	2.46
0.18	31.62	2.22
0.20	34.94	2.01
0.19	35.52	2.01
0.20	35.29	2.06
0.312	11.709	3.506
0.311	16.405	3.422
0.284	20.04	3.401
0.311	20.48	3.292
0.327	24.43	3.163
0.317	28.79	2.456
0.308	28.87	2.987
0.310	32.945	2.660
0.292	33.795	1.788
0.41	12.98	3.39
0.41	16.92	3.25
0.42	18.65	3.55
0.39	21.07	3.98

PLR	Ambient temperature (°C)	COP
0.41	12.98	3.39
0.41	16.92	3.25
0.42	18.65	3.55
0.39	21.07	3.98
0.41	21.18	3.24
0.42	25.92	3.10
0.410	31.35	2.772
0.414	31.53	2.804
0.41	33.85	2.60
0.452	15.11	3.586
0.437	18.13	3.921
0.431	20.03	3.556
0.446	26.53	3.162
0.447	30.80	2.820
0.455	34.870	2.392
0.531	18.14	3.611
0.537	21.87	3.922
0.532	31.56	2.807
0.542	28.07	2.836
0.660	21.65	3.610
0.671	22.29	3.140
0.646	23.43	3.660